JOURNAL OF Applied Polymer SCIENCE

A Novel Electrochemically and Thermally Stable Polythiophene for Photovoltaic Application

Muddasir Hanif, Lijian Zuo, Quanxiang Yan, Xiaolian Hu, Minmin Shi, Hongzheng Chen

MOE Key Laboratory of Macromolecule Synthesis and Functionalization, State Key Lab of Silicon Materials, Department of Polymer Science and Engineering, Zhejiang University, Hangzhou 310027, People's Republic of China

Correspondence to: M. Shi (E-mail: minminshi@zju.edu.cn)

ABSTRACT: Conjugated polymers having good electrochemical and thermal stability are highly desired in optoelectronics. We report a new polythiophene consisting of alternating 4,4′-didodecyl-2,2′-bithiophene and terthiophene units (HPL1) synthesized via Stille coupling reaction. The optical band gap of HPL1 (1.92 eV) is similar to that of regioregular poly(3-hexylthiophene) (rr-P3HT, 1.89 eV). In comparison to rr-P3HT, the HPL1 when subjected to the cyclic voltammetry as thin film shows much superior electrochemical stability and a lower highest occupied molecular orbital energy level (−4.87 eV for rr-P3HT and −4.95 eV for HPL1). The transient photoluminescence study of HPL1 and rr-P3HT shows that both materials have two exciton decay processes, and the excitons of rr-P3HT are quenched more quickly. The onset decomposition, T_d for rr-P3HT (465°C) is 4°C lower than HPL1 (469°C). Preliminary photovoltaic study disclosed that the polymer solar cell based on HPL1:[6,6]-phenyl-C_{61}-butyric acid methyl ester blend showed a power conversion efficiency of 0.63%, with a V_{oc} of 0.6 V, and a short circuit current (J_{sc}) of 2.79 mA cm^{-2} under AM 1.5 illumination (100 mW cm^{-2}). The whole study provided an important example to design new electrochemically and thermally stable polymers with longer exciton life time for application in bulk heterojunction polymer solar cells. © 2012 Wiley Periodicals, Inc. J. Appl. Polym. Sci. 000: 000–000, 2012

KEYWORDS: polymer design; synthesis; electrochemical stability; BHJ solar cell

Received 9 February 2012; accepted 6 April 2012; published online
DOI: 10.1002/app.37852

INTRODUCTION

Solar cells based on organic molecules or conjugated polymers have attracted great attention due to their unique advantages, such as low cost, light weight, flexibility, and facile solution processibility.[1–6] Bulk heterojunction (BHJ) polymer solar cells (PSCs) with conjugated polymers as the electron donor and fullerene derivatives as the electron acceptor are promising candidates for photoinduced charge generation and transport media in solar cells, with power conversion efficiency (PCE) up to 8%.[7–10]An ideal donor polymer has to simultaneously combine strong absorption, small band gap, high hole-mobility, good film-forming properties, and suitable energy levels with respect to the *n*-type material. The two important output parameters namely J_{sc} (short current density) and V_{oc} (open-circuit voltage) in BHJs solar cells make it tricky to find a polymer with a low-band gap to efficiently absorb photons in the visible region of the solar spectrum, while maintaining a high V_{oc} in the solar cells.[11] Decreasing the band gap means that either the highest occupied molecular orbital (HOMO) of the conjugated polymer is raised or the lowest unoccupied molecular orbital (LUMO) is lowered. A raised HOMO energy level gives a lower photovoltage of the device and a lowered LUMO energy level decreases the offset to the LUMO energy level of the *n*-type material used. An offset of ~0.3 eV is required to maintain a sufficient driving force for exciton dissociation and prevents recombination of photogenerated charges.[12] Therefore, it is crucial to design and synthesize polymers with energy levels with suitable LUMO energy level of an electron acceptor to minimize the LUMO energy level difference between donor and acceptor to keep enough driving force for charge generation, thereby maximizing photovoltage in the solar cells.

In this report, we present a novel polythiophene namely HPL1 containing alternating 4,4′-didodecyl-2,2′-bithiophene and terthiophene units. The design, using D–D segments in the polymer backbone, decreases the alkylchain distribution and creates planarity of the backbone. The backbone of the copolymer

Additional Supporting Information may be found in the online version of this article.

HPL1 is exactly the same as that of regioregular poly(3-hexylthiophene) (rr-P3HT), but it shows superior electrochemical, thermal stability, and longer exciton lifetime. Preliminary photovoltaic (PV) property of HPL1 blended with [6,6]-phenyl-C_{61}-butyric acid methyl ester (PCBM) as electron acceptor was also investigated, and it showed a larger V_{oc} than the P3HT:PCBM system under the same device fabrication conditions. The HPL1 can serve as a good example of how the molecular structure influences optical, electronic, electrochemical, and thermal stability performances.

EXPERIMENTAL

Instruments and Materials

^{1}H-NMR spectra were obtained on a Bruker DMX-300 nuclear resonance spectroscope. UV–visible absorption spectra were recorded on a Shimadzu UV-2450 spectrophotometer. Elemental analysis was carried out on a LECO 932 CHNS elemental analyzer. The molecular weight of polymers was determined on a Waters 1525/2414 gel permeation chromatography (GPC), using tetrahydrofuran (THF) as the eluent at room temperature and polystyrene as the internal standard. Thermogravimetric analysis (TGA) curves were measured on Wind Chill Temperature-2 (WCT-2) thermal balance. The time-resolved photoluminescence studies were performed using time-correlated photon-counting apparatus, and the decays were recorded on a combined Edinburgh FLS920 steady-state and lifetime spectrometer. Cyclic voltammetry (CV) was done on a CHI600A electrochemical workstation with Pt disk coated by a polymer film, Pt plate, and standard calomel electrode (SCE) as working electrode, counter electrode, and reference electrode, respectively, in a 0.1 molL^{-1} tetrabutylammonium hexafluorophosphate in dry CH_3CN solution. The CV curve was recorded versus the potential of SCE, which was calibrated by the ferrocene/ferrocenium (Fc/Fc^+) redox couple (4.8 eV below the vacuum level).

The chemicals rr-P3HT (Aldrich, 698989), tris(dibenzylideneacetone)dipalladium (0) (Aldrich, 328774), tri(*o*-tolyl)phosphine (Aldrich, 287822), trimethyltin chloride (Aldrich, 375187), 1,2-dichlorobenzene (Aldrich, 240664), *n*-butyllithium (Acros, 378931000), and toluene (Acros, 326980010) were used as received. All the solvents were freshly purified/distilled prior to use.

Synthesis of Monomers and Copolymer

The monomers 5,5′-dibromo-4,4′-didodecyl-2,2′-bithiophene (DBDDBTH)[13] and 5,5″-bis(trimethylstannyl)-2,2′:5′,2″-terthiophene[14,15] were synthesized according to literature procedures and their ^{1}H-NMR spectra (Supporting Information Figures SEI-1 and SEI-2) are reported. The polymer HPL1 was synthesized by well-known palladium-catalyzed Stille coupling reaction, which is described in details below:

Monomer DBDDBTH (660 mg, 1 mmol), monomer 5,5″-bis(-trimethylstannyl)-2,2′:5′,2″-terthiophene (574 mg, 1 mmol), $Pd_2(dba)_3$ (50 mg), and P(*o*-tolyl)$_3$ (50 mg) were dissolved in a degassed anhydrous toluene (20 mL). The reaction mixture was heated at 85°C under N_2 for 3 days and was cooled to room temperature and poured into 100 mL methanol. The solid obtained was subjected to purification; by washing with water,

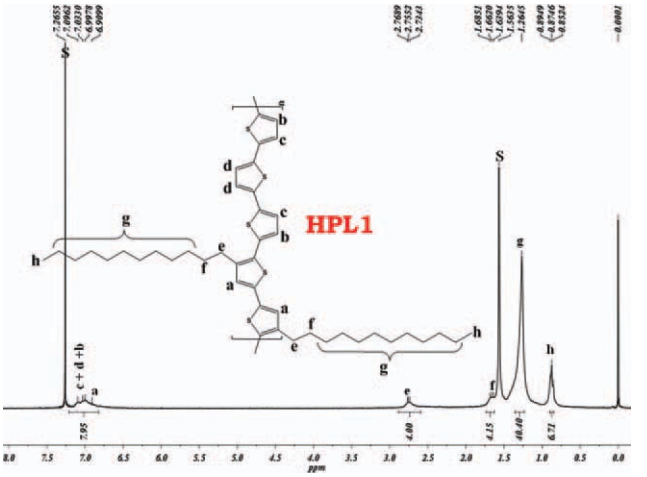

Figure 1. ^{1}H-NMR ($CDCl_3$) of the HPL1, peaks labeled S are solvent peaks. [Color figure can be viewed in the online issue, which is available at wileyonlinelibrary.com.]

extraction with diethyl ether, acetone, ethanol, chloroform to remove small molecules and adsorbed water. Finally, the polymeric material was extracted with purified and dry dichlorobenzene. To get better purification, the polymer in dichlorobenzene was passed through a thin glass column containing Bio-Beads (S-X1, 200–400 mesh, catalog # 152–2150, benzene swelling 7.4 mLg^{-1}). The solvent was then removed under vacuum and dried by mild heating under vacuum and N_2 flow. The polymer was obtained as a dark solid (200 mg, yield 25%).

^{1}H-NMR (300 MHz, $CDCl_3$): δ 7.09 (brs, ArH), 7.03 (brs, ArH), 6.99 (brs, ArH), 6.90 (brs, ArH), 2.76–2.73 (brt, H_e), 1.68–1.63 (brt, H_f), 1.26 (brs, H_g), 0.89–0.85 (brt, H_h). FTIR (KBr pellets, cm^{-1}): 3059 (=C—H, arom. str.), 2921, 2851 (aliph. —CH_2 str.), 1744, 1648, 1541, 1457 (C—S, C=C ring str.), 784, 824 (arom. =C—H oop. vib.). Elemental Analysis: $(C_{44}H_{58}S_5)_n$: Calcd. C 70.72, H 7.82, S 21.46; Found, C 70.71, H 7.80, S 21.44. GPC: M_w = 14.33 K, M_n = 10.57 K, PDI = 1.35. TGA: T_d = 469°C.

Photovoltaic Device Fabrication and Characterization

PSCs were fabricated with indium tin oxide (ITO) glass as the anode, Al as the cathode, and a blended film of polymer: PCBM between the two electrodes as the photoactive layer. The ITO glass was precleaned and poly(3,4-ethylenedioxythiophene):poly(styrenesulfonate) (PEDOT:PSS; Baytron P 4083, Germany) in 30 nm thickness was spin-coated on the ITO substrate. Then, a 20 mgmL^{-1} solution of polymer and PCBM (1 : 1, w/w) in *ortho*-dichlorobenzene (ODCB) was spin-cast at 1000 rpm for 30 s onto the PEDOT : PSS layer. The thickness of the photoactive layer is in the range of 50–70 nm (calibrated by an Ambios Technology XP-2 profilometer). At last, a 100-nm thick Al film was deposited on the photoactive layer under vacuum of 4 × 10^{-4} Pa. The active area of PSCs is 9 mm^2. *I–V* characteristics of the devices in the dark and under illumination of a Thermal Oriel solar simulator with AM 1.5 solar irradiation (100 mW cm^{-2}) were recorded on a semiconductor parameter analyzer (Keithley 2400-SCS), and the light intensity was

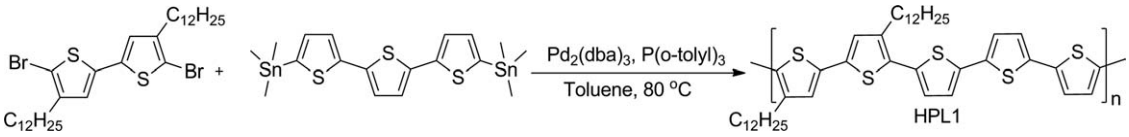

Scheme 1. Synthetic route to HPL1.

calibrated with a PV silicon reference cell. Topographic images of the films were obtained on a Veeco MultiMode atomic force microscopy (AFM) in the tapping mode using an etched silicon cantilever at a nominal load of 2 nN, and the scanning rate for a 4 × 4 μm^2 image size was 1.5 Hz.

RESULTS AND DISCUSSION

Polymer Design, Synthesis, and Characterization

Inspired by the rr-P3HT and the photochemical stability of the thiophene,[16–18] we made a new polymer with good oxidative, electrochemical, and thermal stabilities. The purified monomer of DBDDBTH was copolymerized with 5,5″-bis(trimethylstannyl)-2,2′:5′,2″-terthiophene resulting in HPL1 (Scheme 1). The D–D thiophene units are good electron donating groups, capable of decreasing the band gap through planarity, and bond length alternation.[19] The dodecyl side-chains were attached at the three-position of the bithiophene rings, to maintain the solubility and high degree of order in the solid state. For the polymerization reaction, the Stille coupling reaction was used, and no end-capping agents were used after the polymerization.

Molecular weight distribution of the polymer was determined by the size-exclusion chromatography (GPC). As presented in Table I, the weight-average (M_w) and number-average molecular weights (M_n) of HPL1 (Supporting Information Figure SEI-3) are 14,333 and 10,574 g mol^{-1}, respectively. The polydispersity index (M_w/M_n) is 1.35, consistent with a polycondensation reaction. The polymer was further characterized by ^{1}H-NMR and FTIR.

The ^{1}H-NMR (Figure 1) of the polymer HPL1 in $CDCl_3$ showed the aromatic region for thiophenes. The three broad peaks at 7.09, 7.03, and 6.99 ppm were observed for the aromatic hydrogen of terthiophenes H_c, H_d, and H_b. The peak at 6.90 ppm was observed for the lonely aromatic hydrogen H_a of the 4,4′-didodecyl-2,2′-bithiophene unit in the HPL1.

In the aliphatic region, broad triplet was observed between 2.76 and 2.73 ppm attributed to H_e which is closest to the thiophene ring. The broad multiplet between 1.68 and 1.63 ppm was observed for H_f. The tall sharp peak at 1.26 ppm can be attributed to the H_g, and the last triplet between 0.89 and 0.85 ppm can be attributed to the terminal CH_3 groups.

As the polymer HPL1 consists of terthiophene and 4,4′-didodecyl-2,2′-bithiophene units, it is logical, as a reference to compare FTIR spectra of terthiophene and DBDDBTH with the FTIR spectrum of HPL1 (Figure 2, Table II).

Table I. Molecular Weight Comparison Between HPL1 and rr-P3HT

Polymers	M_w	M_n	PDI
HPL1	14,333[a]	10,574[a]	1.35[a]
P3HT	17,000[b]	13,076[b]	1.30[b]

[a] Data from GPC (THF), [b] Commercial *rr*-P3HT.

FTIR analysis[20] (Figure 2, Table II) indicates the aromatic hydrogen str. (=C—H) at 3067 cm^{-1} for terthiophene, 3054 cm^{-1} for DBDDBTH, and 3059 cm^{-1} for the polymer HPL1. The aliphatic —CH_2 str. were observed for DBDDBTH at 2917, 2851 cm^{-1} and 2921, 2851 cm^{-1} for the polymer HPL1. The C=C ring str. (thiophene) were observed at 1743, 1644, 1516, and 1422 cm^{-1} for terthiophene, 1739, 1647, 1534, and 1408 cm^{-1} for DBDDBTH, and 1744, 1648, 1541, and 1457 cm^{-1} for HPL1. The Aromatic =C—H (thiophene ring) out of plane (oop) vibrations for terthiophene were observed at 833, 801, 796, and 691 cm^{-1}. Similar, oop vibrations for thiophene rings in the polymer HPL1 were observed at 824 and 784 cm^{-1}.

Optical Properties

The UV–vis absorption spectra of two polymers HPL1 and rr-P3HT in ODCB solution and film are given in Figure 3(a, b) respectively. The UV–vis absorption spectra in ODCB solution for the rr-P3HT and HPL1 show a broad band at 451 and 484 nm, respectively. The rr-P3HT film [Figure 3(b)] shows peaks at 524, 555, and 602 nm, which originate from the high degree of three-dimensional order in the solid state of rr-P3HT and are indicative of microcrystalline polymer structure.[16,17] Similarly, the HPL1 in film shows 2 peaks at 547 and 587 nm, showing the presence of ordered structure in the solid-state. From the onset wavelengths [Figure 3(b)], the optical band gap was estimated to be 1.89 eV for rr-P3HT and 1.92 eV for HPL1 (Table III). To have a deeper insight into the exciton formation and decay, the transient photoluminescence of HPL1 and rr-P3HT was measured and compared (Figure 4), and the results are summarized in Table IV.

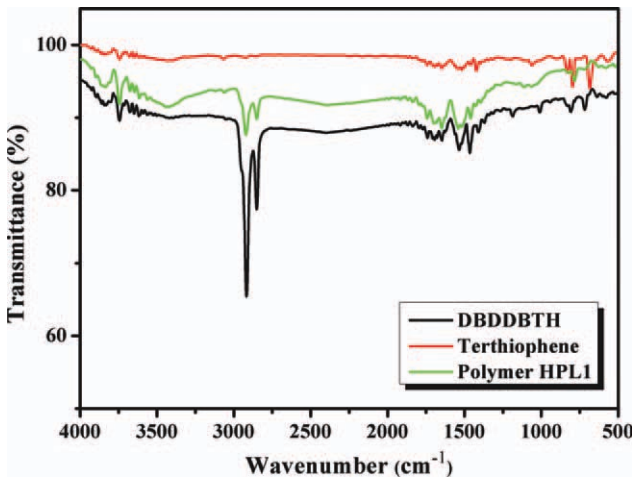

Figure 2. FTIR spectra (KBr pellet) of the monomers and the polymer HPL1. [Color figure can be viewed in the online issue, which is available at wileyonlinelibrary.com.]

Table II. FTIR Peaks Assignments for the Monomers and the Polymer HPL1

Functional group	Terthiophene (cm^{-1})	DBDDBTH (cm^{-1})	HPL1 (cm^{-1})
=C—H (arom. Str.)	3067	3054	3059
Aliphatic —CH str.	Nil	2917, 2851	2921, 2851
C=C ring str. (thiophene)	1743, 1644, 1516, 1422	1739, 1647, 1534, 1408	1744, 1648, 1541, 1457
C—H oop vib.	833, 801, 796, 691	826, 809, 717	824, 784

It is evident from Figure 4 that the excitons of rr-P3HT decay more quickly in comparison to the HPL1. The exciton lifetime of HPL1 is 5.344 ns, longer than that of rr-P3HT (4.908 ns). Both materials have two decay processes. The more is the life time of an exciton, the more is the chance for its diffusion and dissociation to produce current, therefore, HPL1 should be more suitable in comparison to the rr-P3HT for the BHJ blends used in the solar cells.

Thermal Properties

The thermal stability of the HPL1 and rr-P3HT was investigated by TGA under the nitrogen atmosphere. Both the polymers display (Figure 5) good thermal stability with onset decomposition, T_d = 465°C for rr-P3HT and 469°C for HPL1. HPL1 not only shows 4°C higher T_d but also shows better stability during the decomposition above 635°C, which is rare quality for non-fluorinated compounds. Good thermal stability of the two polymers can be explained by good packing properties.

Electrochemical Properties

In the cyclic voltammetry experiment, a voltage (potential) is applied (cycled) to a working electrode in solution and current flowing at the working electrode is plotted versus the applied voltage to give the cyclic voltammogram (CV).[21] The CVs in CH_3CN were recorded for the two polymers rr-P3HT and HPL1 as shown in Figure 6(a, c) (positive and negative scans), respectively, and their electrochemical properties are summarized in Table V. The CVs [Figure 6(a, c)] of the two polymers show that both rr-P3HT and HPL1 are good electron donors and

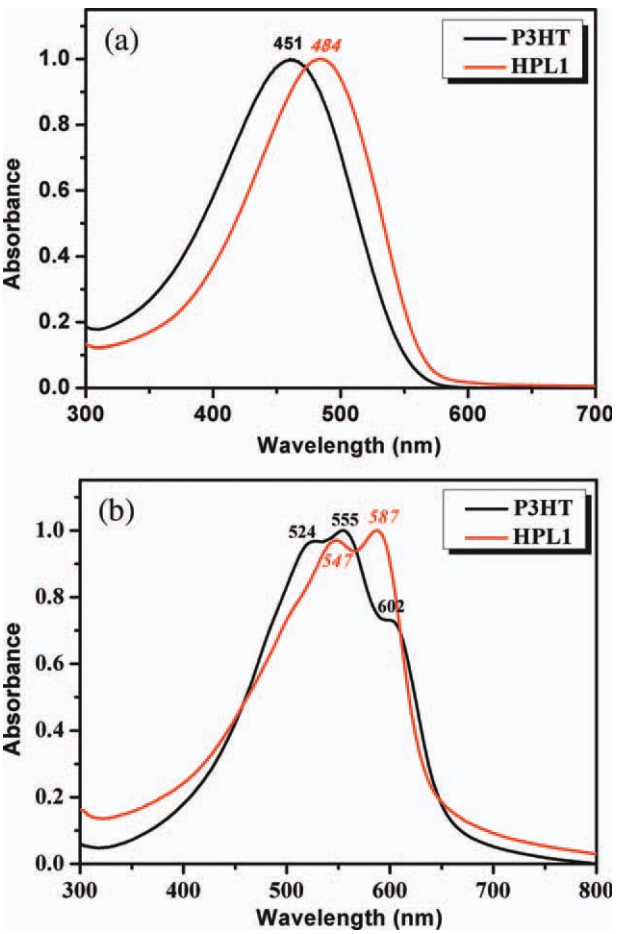

Figure 3. UV–vis absorption spectra of HPL1 and rr-P3HT in dichlorobenzene solution (a) and film (b). [Color figure can be viewed in the online issue, which is available at wileyonlinelibrary.com.]

Table III. Optical Properties Comparison Between HPL1 and rr-P3HT

λ_{max} (sol, nm)	λ_{max} (film, nm)	E_g^{opt} (eV)
[a]484	[b]548, 588	[b]1.92
[a]451	[b]524, 555, 602	[b]1.89

[a] From Fig. 3a (ODCB solution), [b] 3b (spin-coated film).

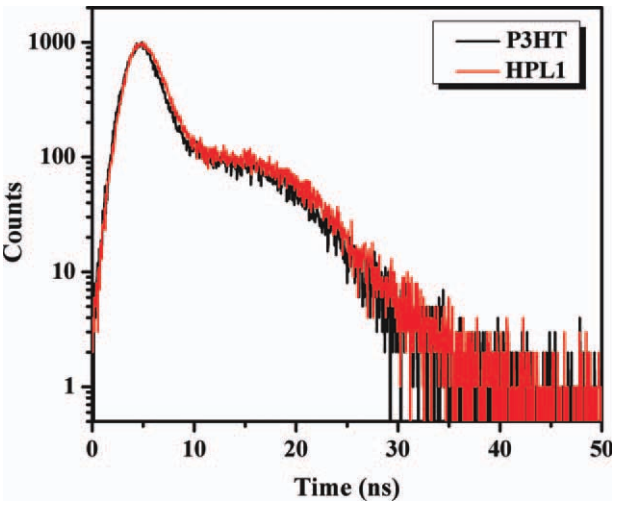

Figure 4. Transient photoluminescence characterization of HPL1 and rr-P3HT in ODCB solution. [Color figure can be viewed in the online issue, which is available at wileyonlinelibrary.com.]

Table IV. The Tail-Fit Time Data from the Curve in Figure 2

Samples	τ_1 (ns)	τ_2 (ns)	τ (ns)
P3HT	1.19	6.97	4.908
HPL1	1.15	7.22	5.344

show reversible oxidation (*p*-doping and dedoping) processes. The HPL1 shows much better reduction process (*n*-doping and dedoping peak currents) as compared with the rr-P3HT.

The onset oxidation-potential (vs. SCE) E_{ox} is 0.47 V for rr-P3HT and 0.55 V for HPL1. From the oxidation potential values, the HOMO levels of the two polymers can be estimated using the equation [$E_{HOMO} = -(E_{ox} + 4.4)$ eV].[22] The HOMO energy level for rr-P3HT is −4.87 eV which is in good agreement with previously reported −4.76 eV by Yongfang Li et al.[23] and −4.8 eV by Boer et al.[24] The HOMO energy level for HPL1 is −4.95 eV. The position of the HOMO energy level of a *p*-type polymer is of great importance when evaluating the materials from a solar cell perspective. The HPL1 has deeper (0.08 eV) HOMO level than rr-P3HT, which helps to enhance the V_{oc} and oxidative stability of the polymer [$V_{oc} = E_{LUMO}$ (acceptor) – E_{HOMO} (donor) – 0.3 V].[25] Similarly, the reduction-potential E_{red} for rr-P3HT is −0.93 V (vs. SCE) and −0.80 V for HPL1. From the reduction potential values, the LUMO levels of the two polymers can be estimated using the equation [$E_{LUMO} = -(E_{red} + 4.4)$ eV]. Therefore, the LUMO levels for rr-P3HT and HPL1 are −3.47 and −3.6 eV, respectively.

For the longer life of a solar cell, the oxidative stability of a donor (*p*-type) polymer is of high importance. Therefore, we subjected the thin films of rr-P3HT and HPL1 to repeated positive scans using cyclic voltammetry (20 cycles). If we compare Figure 3(b, d), we can find that the positive current for the *p*-doping and dedoping remains almost constant (compare the first and 20th cycles) for the HPL1, while rr-P3HT shows evident decrease in the positive current for the *p*-doping and dedoping

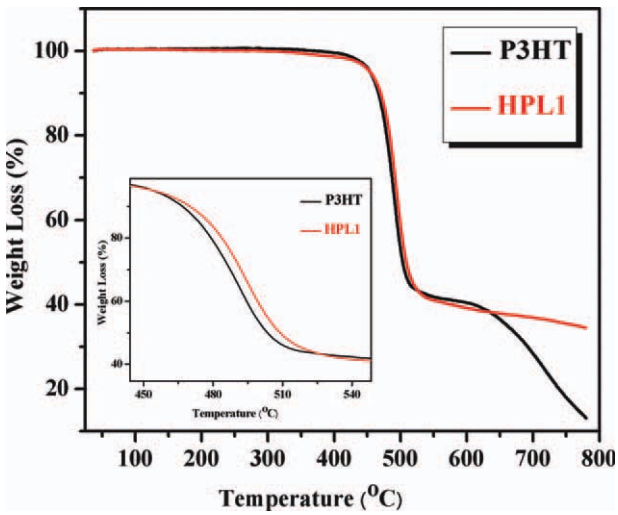

Figure 5. TGA curves of rr-P3HT and HPL1. [Color figure can be viewed in the online issue, which is available at wileyonlinelibrary.com.]

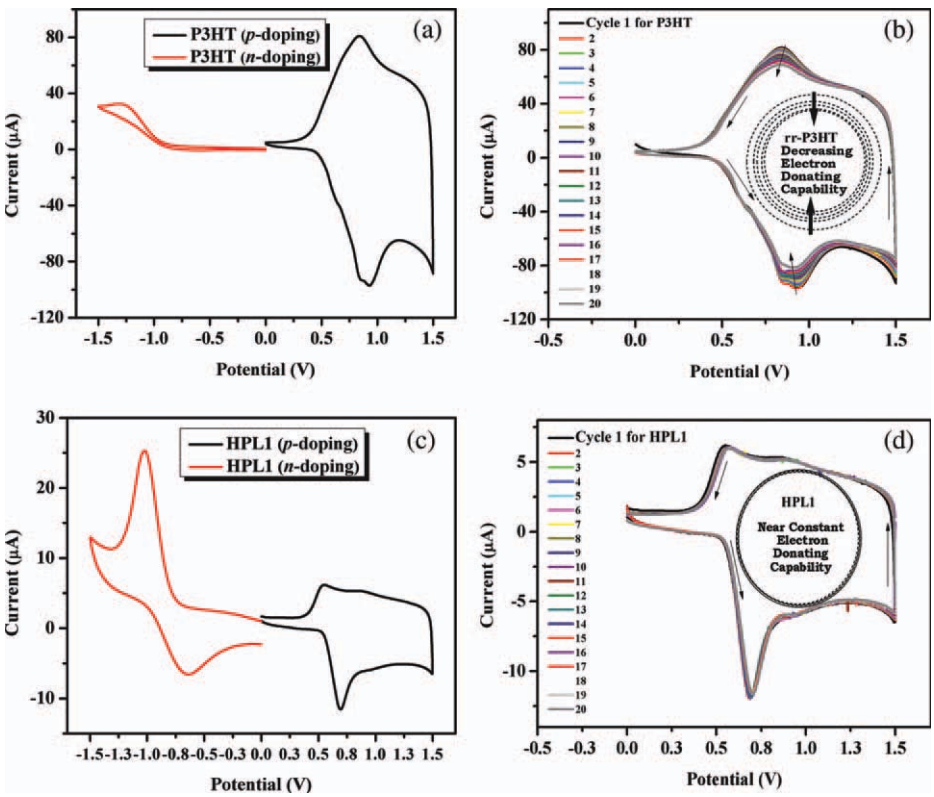

Figure 6. Electrochemical voltammograms measured for polymer films [rr-P3HT (a and b) and HPL1 (c and d)] by CV. [Color figure can be viewed in the online issue, which is available at wileyonlinelibrary.com.]

Table V. Electrochemical Results from Cyclic Voltammetry of Polymer Films

Polymers	E_{ox}[a] (V)/*HOMO*[b] (eV)	E_{red}[a] (V)/*LUMO*[b] (eV)	E_g^{ec}[c] (eV)
P3HT	0.47/−4.87	−0.93/−3.47	1.4
HPL1	0.55/−4.95	−0.80/−3.6	1.35

[a] Onset-peak potentials versus SCE, [b] Energy levels are estimated from HOMO/LUMO = $-(E^{ox/red} + 4.4)$ eV, [c] Electrochemical band gap.

process. This clearly shows that the HPL1 might be a better candidate in comparison to the widely used rr-P3HT to get longer durability when used as a *p*-type material in BHJ polymer solar cell.

The electrochemistry[21] defines current as $i = dQ/dt$, where Q is charge and t is time. When an organic molecule is subjected to the positive scan in the cyclic voltammetry, the molecule may undergo two kinds of processes in one cycle. First, the removal of electron (at a certain potential) simply known as oxidation and the observation of anodic peak current i_{pa}. The first process changes the molecule from neutral to positive (*p*-doping). Second, the *p*-doped molecule accepts electron, undergoes reduction (*p*-dedoping) and the observation of cathodic peak current i_{pc}. The second process changes the molecule from positive to neutral. If the redox process is not very efficient, the molecule may remain oxidized or undergo other changes which are reflected as the loss of current with increasing number of cycles.[26]

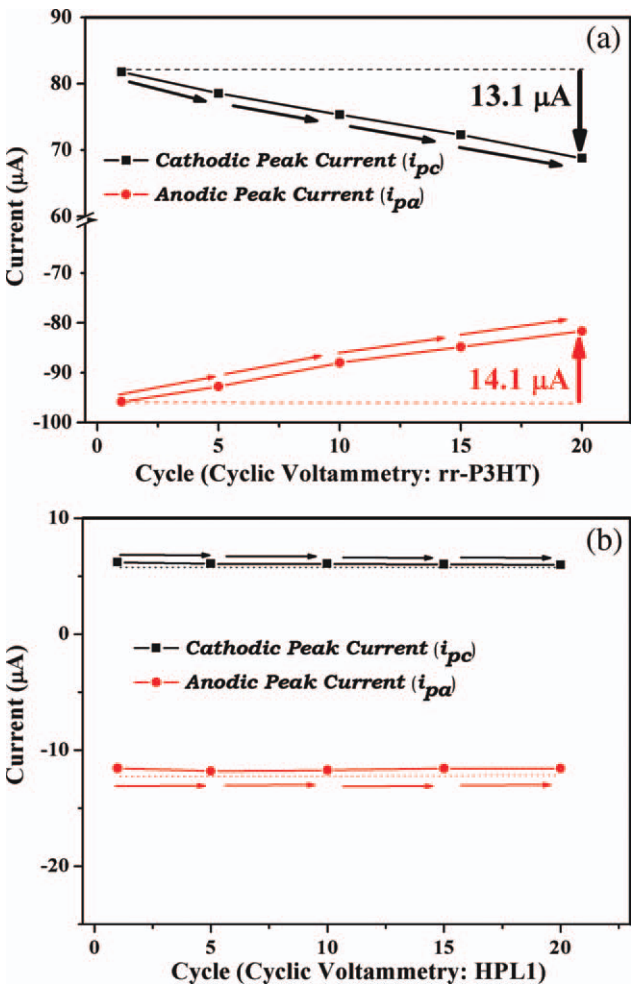

Figure 7. Electrochemically measured currents (20 cycles) for the polymer films [rr-P3HT (a) and HPL1 (b)] by CV. [Color figure can be viewed in the online issue, which is available at wileyonlinelibrary.com.]

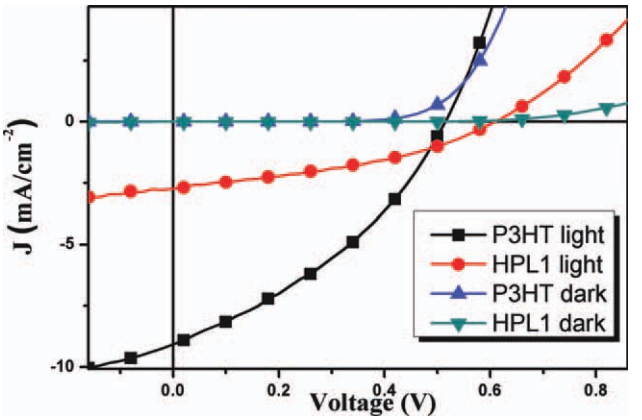

Figure 8. *J–V* curves for the solar cells made from the rr-P3HT and HPL1. [Color figure can be viewed in the online issue, which is available at wileyonlinelibrary.com.]

In a polymer-based solar cell, the polymer is a *p*-type donor of electron to the acceptor (PCBM) and the source of current produced by the solar cell.[6] Therefore, the ability to produce same current with increasing number of cycles is very important. We have compared the anodic and cathodic peak currents (i_{pa} and i_{pc}) values (20 cycles) for the thin films of the rr-P3HT and HPL1. The comparison shows 14.1 μA decrease [Figure 7(a)] of anodic peak current for rr-P3HT from the initial value after 20 cycles, while no significant decrease in current was observed for HPL1 [Figure 7(b)]. This fact clearly demonstrates the decreasing electron donating capability of rr-P3HT and near constant electron donating capability of HPL1. For deeper understanding the coulometric, electrochemical, and device-based properties will be reported in future.

Photovoltaic Properties

To evaluate the PV property of the polymers HPL1 and rr-P3HT, PSCs were fabricated with the device structure of ITO/PEDOT : PSS/polymer : PCBM (1 : 1, w/w)/Al. Figure 8 shows the *J–V* curves of the PSCs under the illumination of AM 1.5

Table VI. Solar-Cell Parameters Comparison for the HPL1 and rr-P3HT

Polymers	Ratio	J_{SC} (mA cm^{-2})	V_{oc} (V)	FF	η (%)
P3HT	1 : 1	9.229	0.52	34.96	1.677
HPL1	1 : 1	2.795	0.6	37.5	0.625

Polymer : PCBM = 1 : 1, w/w in ODCB.

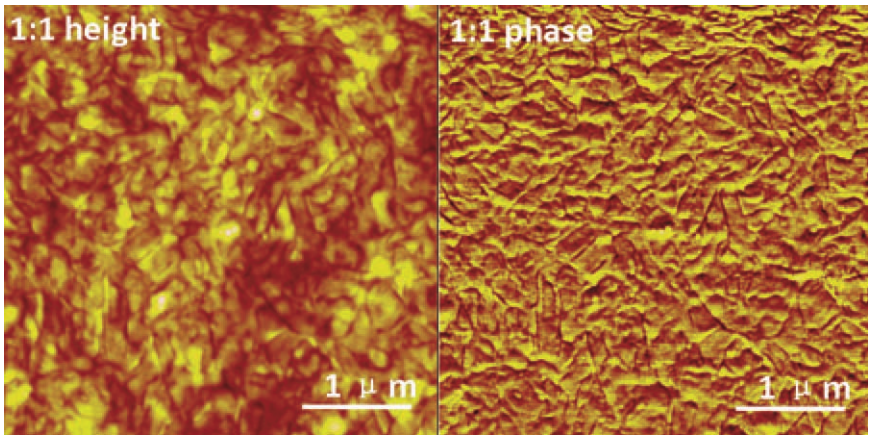

Figure 9. AFM images of the HPL1 : PCBM (1 : 1, w/w) film. [Color figure can be viewed in the online issue, which is available at wileyonlinelibrary.com.]

solar irradiance (100 mW cm^{-2}), and the corresponding PV data are summarized in Table VI. Preliminary PV study disclosed that the PSC based on HPL1 : PCBM = 1 : 1 blend showed a PCE of 0.63%, with a V_{oc} of 0.6 V, short circuit current (J_{sc}) of 2.79 mA cm^{-2} and fill factor (FF) of 0.6. Although the efficiency of HPL1 with the PCBM blend is lower than the rr-P3HT but still HPL1 shows higher V_{oc} (as predicted from CV) and FF. The surface morphology of the blended film of HPL1 : PCBM (1 : 1, w/w) was observed by AFM (Figure 9).

The blended film shows a relatively rough surface and large phase-separated domains (more than 50 nm), suggesting that the morphology of the blended film needs further optimizations to achieve better PV performance.[27]

CONCLUSIONS

A new polythiophene namely HPL1, containing alternating terthiophene and 4,4′-didodecyl-2,2′-bithiophene, is synthesized via Stille coupling reaction. The optical band gap of the HPL1 (1.92 eV) is similar to that of rr-P3HT (1.89 eV). The new polymer possessed lower HOMO, LUMO levels (closer to the ideal polymer),[28] longer exciton lifetime, superior electrochemical stability, and higher thermal stability in comparison to that of rr-P3HT. Preliminary PV study disclosed that the PSC based on HPL1:PCBM blend showed a PCE of 0.63%, with a V_{oc} of 0.6 V, and a short circuit current (J_{sc}) of 2.79 mA cm^{-2} under AM 1.5 illumination (100 mW cm^{-2}). Although the efficiency of the HPL1 with the PCBM blend is lower than that of rr-P3HT but the HPL1 shows higher V_{oc} and FF. Therefore, further device optimization can increase the PCE of the solar cell.

ACKNOWLEDGMENTS

This work was supported by the National Natural Science Foundation of China (Nos. 50990063, 51011130028, and 51073135) and Zhejiang Province Natural Science Foundation (No. Y407101). The work was also partly supported by Developing Program of Zhejiang Province Key Scientific and Technical Innovation Team (No. 2009R50004).

REFERENCES

1. Hu, X. L.; Shi, M. M.; Chen, J.; Zuo, L. J.; Fu, L.; Chen, H. Z. *Macromol. Rapid Commun.* **2011,** *32*, 506.
2. Dennler, G.; Scharber, M. C.; Brabec, C. J. *Adv. Mater.* **2009,** *21*, 1323.
3. Gunes, S.; Neugebauer, H.; Sariciftci, N. S. *Chem. Rev.* **2007,** *107*, 1324.
4. Helgesen, M.; Søndergaard, R.; Krebs, F. C. *J. Mater. Chem.* **2010,** *20*, 36.
5. Boudreault, P. T.; Najari, A.; Leclerc, M. *Chem. Mater.* **2011,** *23*, 456.
6. Hains, A. W.; Liang, Z. Q.; Woodhouse, M. A.; Gregg, B. A. *Chem. Rev.* **2010,** *110*, 6689.
7. Chen, H. Y.; Hou, J. H.; Zhang, S. Q.; Liang, Y. Y.; Yang, G. W.; Yu, L. P.; Yang, Y.; Wu, Y.; Li, G. *Nat. Photon.* **2009,** *3*, 649.
8. Liang, Y. Y.; Xu, Z.; Xia, J. B.; Tsai, S. T.; Wu, Y.; Li, G.; Ray, C.; Yu, L. P. *Adv. Mater.* **2010,** *22*, E135.
9. Chu, T. Y.; Lu, J. P.; Beaupré, S.; Zhang, Y. G.; Pouliot, J. R.; Wakim, S.; Zhou, J. Y.; Leclerc, M.; Li, Z.; Ding, J. F.; Tao, Y. J. *Am. Chem. Soc.* **2011,** *133*, 4250.
10. Zhou, H. X.; Yang, L. Q.; Stuart, A. C.; Price, S. C.; Liu, S. B.; You, W. *Angew. Chem. Int. Ed.* **2011,** *50*, 2995.
11. Thompson, B. C.; Frechet, J. M. *Angew. Chem. Int. Ed.* **2008,** *47*, 58.
12. Peet, J.; Kim, J. Y.; Coates, N. E.; Ma, W. L.; Moses, D.; Heeger, A. J.; Bazan, G. C. *Nat. Mater.* **2007,** *6*, 497.
13. Takahashi, M.; Masui, K.; Sekiguchi, H.; Kobayashi, N.; Mori, A.; Funahashi, M.; Tamaoki, N. J. *Am. Chem. Soc.* **2006,** *128*, 10930.
14. Asawapirom, U.; Guntner, R.; Forster, M.; Farrell, T.; Scherf, U. *Synthesis* **2002,** *9*, 1136.
15. Bao, Z.; Chan, W. K.; Yu, L. J. *Am. Chem. Soc.* **1995,** *117*, 12426.
16. Kim, J. S.; Park, Y.; Lee, D. Y.; Lee, J. H.; Park, J. H.; Kim, J. K.; Cho, K. *Adv. Funct. Mater.* **2010,** *20*, 540.

17. Aryal, M.; Trivedi, K.; Hu, W. W. *ACS Nano* **2009,** *3*, 3085.
18. Manceau, M.; Bundgaard, E.; Carlé, J. E.; Hagemann, O.; Helgesen, M.; Søndergaard, R.; Jørgensen, M.; Krebs, F. C. *J. Mater. Chem.* **2011,** *21*, 4132.
19. Bredas, J. L. *J. Chem. Phys.* **1985,** *82*, 3808.
20. Pavia, D. L.; Lampman, G. M.; Kriz, G. S.; Vyvyan, J. R. In Introduction to Spectroscopy: A Guide for Students of Organic Chemistry, 4th ed.; Brooks/Cole, Cengage Learning: Belmont, CA, **2009.**
21. Bard, A. J.; Faulkner, L. R. Electrochemical Methods: Fundamentals and Applications, 2nd ed.; Wiley: New York, **2001.**
22. Wei, Y. F.; Zhang, Q.; Jiang, Y.; Yu, J. S. *Macromol. Chem. Phys.* **2009,** *210*, 769.
23. Hou, J. H.; Tan, Z. A.; Yan, Y.; He, Y. J.; Yang, C. H.; Li, Y. F. *J. Am. Chem. Soc.* **2006,** *128*, 4911.
24. Asadi, K.; Gholamrezais, F.; Smiths, E. C. P.; Blom, P. W. M.; Boer, B. D. *J. Mater. Chem.* **2007,** *17*, 1947.
25. Scharber, M. C.; Mühlbacher, D.; Koppe, M.; Denk, P.; Waldauf, C.; Heeger, A. J.; Brabec, C. J. *Adv. Mater.* **2006,** *18*, 789.
26. Baba, A.; Park, M.-K.; Advincula, R. C.; Knoll, W. *Langmuir* **2002,** *18*, 4648.
27. Sundarrajan, S.; Murugan, R.; Nair, A. S.; Ramakrishna, S. *Mater. Lett.* **2010,** *64*, 2369.
28. Zhou, H.; Yang, L.; Stoneking, S.; You, W. *Appl. Mater. Interfaces* **2010,** *2*, 1377.